Journal of Engineering Physics and Thermophysics, Vol. 74, No. 3, 2001

CERTAIN ASPECTS OF COMPUTER SIMULATION OF HYPERSONIC FLOWS: STABILITY, NONUNIQUENESS, AND BIFURCATION OF NUMERICAL SOLUTIONS OF THE NAVIER–STOKES EQUATIONS

G. A. Tarnavskii and S. I. Shpak UDC 519.6:531.332.533.6

A number of problems associated with the nonuniqueness of numerical solutions of the Navier–Stokes equations used for simulating processes of a hypersonic real gas flow past blunt bodies are considered. The processes of evolution of a stationary pattern of flow perturbed by a single pulse at an initial time instant are considered at different values of the governing parameters of the problem. The instability of the bifurcation type resulting in transition of the nonstationary process from one branch of solution to another and the attainment of a stationary regime is investigated.

The development of computer technology and the associated advances in computer simulation in problems of gas dynamics in the field of numerical investigation of complex flows, the possibility of performing multiparametric cycles of calculation with a detailed fine-step variation of governing parameters, in particular, for the problems of external flow past differently shaped bodies, such as the Mach and Reynolds numbers of a free stream, the temperature factor, the efficient specific heat ratio, etc., and the practice of storage in databases and subsequent joint analysis of the results of the cycles of these calculations make it possible to study, on a qualitatively new level, the problem concerning the degree of the reliability of the numerical solutions obtained as a problem of the adequacy of a mathematical model and of the algorithms and codes implementing it to the occurring physical process. One of the important and generally little studied aspects of this problem is the nonuniqueness of numerical solutions of nonlinear systems of the differential equations of gas dynamics. This, in turn, involves the problems of the stability of flows with shock waves and of the shock waves themselves in gases, especially with account for their real properties, against different kinds of perturbations. Generally speaking, investigation of the stability of shock waves has been the concern of a large number of analytical computational, and experimental works, a review of which (even a brief one) is difficult. In the present work, we consider these problems in a somewhat different vein and from somewhat different positions that differ rather substantially from the traditional ones.

Formulation of the Problem. The present work is an extension of previous investigations [1, 2]. We carried out a large series of computational experiments in the following formulation. We investigated supersonic viscous heat-conducting gas flow past the spherically blunt nose of a cylinder or cone. In the region bounded by an isothermal or thermally insulated surface of the body, bow compression shock (the position and configuration of which were sought in the process of solution), symmetry axis, and by the outlet boundary, we performed numerical integration of a nonstationary system of Navier–Stokes equations, written in a traditional dimensionless form with parameters M_∞, Re_∞, Pr, and γ that determine the solution, by the method [3, 4], of the first and second order of accuracy over time and space, respectively. The system was closed by the quasiequilibrium equation of state written in the form of the equation of state of a perfect gas with a variable value of γ which was determined by the method of "efficient specific heat ratio" [5] that approxi-

Institute of Theoretical and Applied Mechanics, Siberian Branch of the Russian Academy of Sciences, Novosibirsk, Russia; email: shpak@itam.nsc.ru. Translated from Inzhenerno-Fizicheskii Zhurnal, Vol. 74, No. 3, pp. 125–132, May–June, 2001. Original article submitted October 31, 2000.

 1062-0125/01/7403-0710$25.00

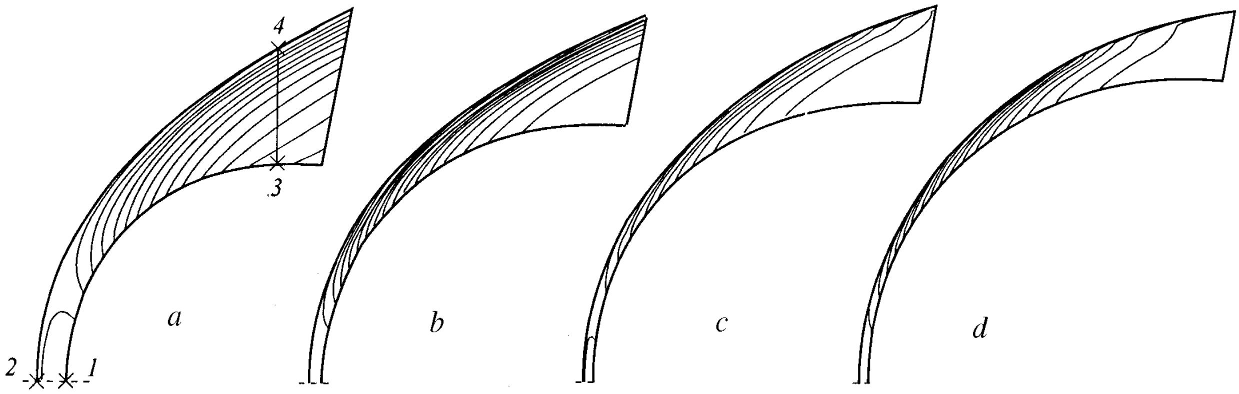

Fig. 1. Isolines of the values of density in a stationary flow pattern.

mately models excitation of internal degrees of freedom in the gas. As the basic scales in nondimensionalization, we used the radius of bluntness R_b, the density ρ_∞, and the free stream velocity U_∞, and the scales of the remaining quantities were obtained from them by means of respective combinations. This uniquely governs the conversion, when required, of the dimensionless quantities, given below, into dimensional ones.

From the side of the external free stream, the stationary pattern of flow (typical patterns are shown in Fig. 1) experiences the incidence of peak-shaped energy release pulses of intensity I and periodicity T with a steep leading front and a large attenuation decrement $E(x, t) = I\delta(\omega t - kx)$, where δ is the unit pulse function (the Dirac wave delta-function)

$$\delta(z) = \begin{cases} 1\,; & z = \pm\, 0, 1, 2, \ldots \\ 0\,; & z \neq \pm\, 0, 1, 2, \ldots\,, \end{cases}$$

and the frequency ω, wave number k, and wavelength L are connected with the parameters T and U_∞ by the relations $\omega = 2\pi/T$, $k = 2\pi/L$, and $L = U_\infty T$. The instant of incidence of the first pulse on the stationary bow shock is taken to be the start of the reading of time. In [2], a nonstationary process of the reorganization of the flow pattern was considered in the time interval $0 \le t \le T$ between the incidences of the first and second pulses on the bow shock. In the present work, we study the process of evolution of the solution perturbed by a single pulse ($T >> T_*$, where T_* is the characteristic time of the process) at the initial instant of the flow field, i.e., mathematically, induced by the change in the initial data of a continuous differential problem or, computationally, by the replacement of the starting conditions for the algorithm of the solution of a discrete problem. Generally speaking, the problems of the equivalence between the continuous differential and discrete finite-difference problems in the presence, in the solution domains, of strong and weak discontinuities have been insufficiently studied, especially in the possible presence of transition regimes in the vicinity of the critical values of governing parameters — the problem to be discussed below when the results of numerical simulation are analyzed. Our main focus of attention is the study of the evolution of flow in the range of parameters between the boundaries of the regimes of weak and strong instabilities [1].

Some Results of Calculations. The model of the efficient specific heat ratio [5] was used to perform a series of calculations in wide ranges of the governing parameters $3 \le M_\infty \le 50$, $1.01 \le \gamma \le 5/3$ with a fairly short step ΔM_∞, $\Delta\gamma$ and to create a specialized division of a database [4] as a reference one for further investigations. Below, as an illustration, we give the results of calculation of thermally insulated bodies immersed in a gas flow with the parameters $M_\infty = 10$, $Re_\infty = 0.25\cdot10^5$, and $Pr = 0.72$.

Figure 1 presents stationary flows near the nose part of the body that were induced at $\gamma = 1.4$ (a), 1.10 (b), 1.07 (c), and 1.037 (d). The figure shows the density isolines undergoing equidistant change from ρ_{max} near the stagnation point to ρ_{min} downstream. One can see a substantial rearrangement of flow with decrease in γ, starting roughly at $\gamma = 1.10$. First, the general configuration of the flow undergoes a change:

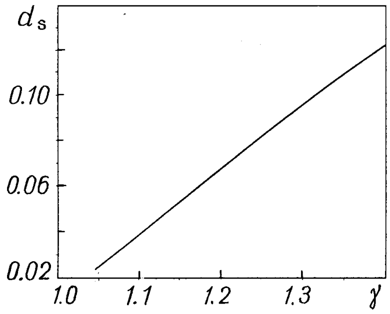

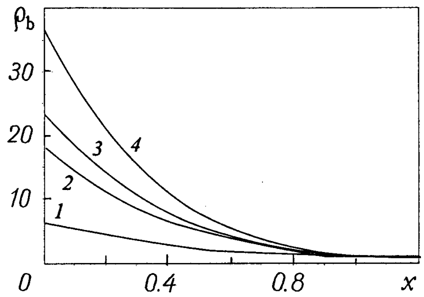

Fig. 2. Dependence of the distance of departure of the front shock from the body at the stagnation line on the specific heat ratio.

Fig. 3. Distribution of density along the body surface. Curves 1, 2, 3, and 4 correspond to the values $\gamma = 1.4$, 1.1, 1.07, and 1.037.

the isochors "converge" both in the direction from the body to the bow compression shock and upstream. A narrow layer with high density and temperature gradients is formed near the bow shock. Second, a large decrease is observed in the thickness of the shock layer, i.e., in the region of the perturbed flow between the bow shock and the body surface: the dependence of the departure of the shock from the body at the line of stagnation $d_s(\gamma)/R_b$ is shown in Fig. 2. We call attention to the practically exact linear dependence of $d_s(\gamma)$ in this range of γ. This is a very interesting fact, just as arc any linear dependences obtained in the solution of substantially nonlinear problems. We note that Fig. 2 represents an integrated analysis of a large number of calculations with parametric sorting of γ (with a small step $\Delta\gamma$ from calculation to calculation), and each point of this graph is a stationary solution of a separate nonstationary problem. Third, the values of density increase enormously in the shock layer and, moreover, at small γ's both transverse (from a shock to the body) and longitudinal (downstream) gradients of the values are very large: Fig. 3 shows the distributions of the density in the boundary layer along the body surface $\rho_b(x)/\rho_\infty$ for different values of γ. The coordinate x is reckoned from the nose of the body (stagnation points) along its axis and is related to the radius of bluntness.

This structure of flow favors the development of the perturbations generated in the flow and the appearance of instabilities in both the region of the bow shock, up to its destruction, and the boundary layer.

To analyze the stability of stationary structures of flow (see Fig. 1) to the perturbations incident from the side of the free stream, similarly to a physical experiment, a "system of probes" was used that were located at points 1–4 (denoted by crosses in Fig. 1a): along the stagnation line on the surface of the body at the stagnation point 1 and at the front of the bow shock 2 and also along the ray perpendicular to the axis of the problem and emanating from the center of the spherical bluntness, correspondingly on the surface of the body 3 and at the front of the bow compression shock 4 at which the values of the gas-dynamical parameters $f(t)$ were steadily tracked at large time intervals (the current values of the density $\rho(t)/\rho_\infty$ will be given in what follows).

Analysis of the results of many computational experiments carried out in a wide range of governing parameters makes it possible to distinguish four basic regimes of the susceptibility of the flow pattern to perturbations: stable, neutrally stable, neutrally stable with transition, and unstable. These regimes can undergo some gradation in a two-parametric region (M_∞, γ): at a certain fixed value of M_∞, the stable regime is realized in the region where $\gamma > \gamma_1$, the neutrally stable regime in the region of $\gamma_2 < \gamma < \gamma_1$; the neutrally stable regime with transition is realized in the very narrow range $\gamma_3 < \gamma < \gamma_2$, and the unstable regime is realized when $\gamma < \gamma_3$. The boundaries of the regimes are rather smeared, i.e., one cannot point to strictly definite values of γ_1, γ_2, and γ_3, since the regimes smoothly change one another. We point to the fact that for $M_\infty < M_*$, where M_* is a certain critical value of M_∞ (see [1]), only stable regimes exist. It should be noted that the developing regimes and correspondingly their boundaries depend on the level of perturbations, which

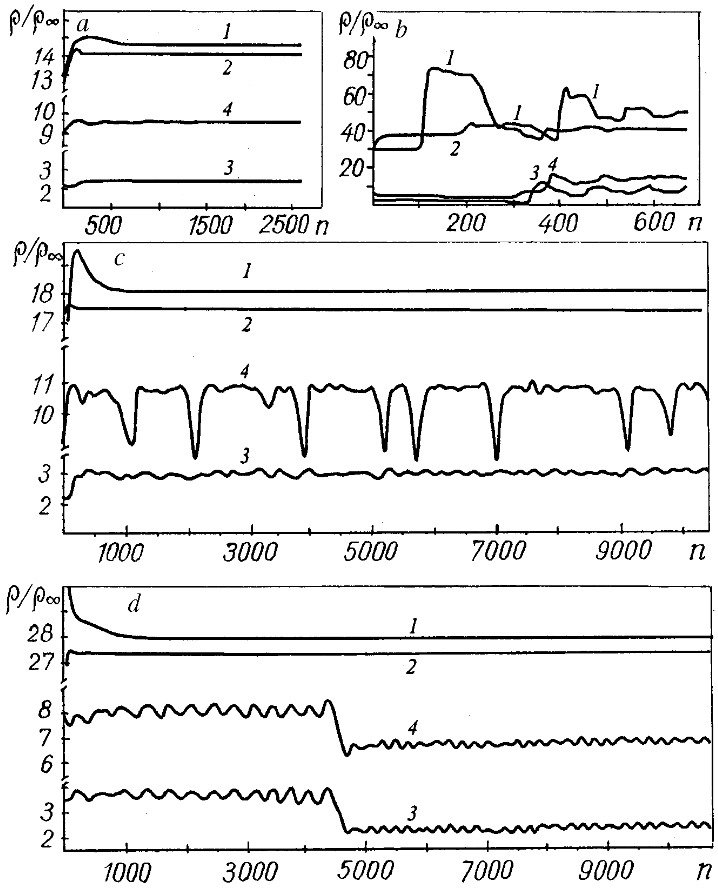

Fig. 4. Evolution of the perturbations of density in time at control points 1–4 (Fig. 1). The values γ = 1.13 (a) 1.03 (b), 1.1 (c), and 1.055 (d).

were selected to be small but finite (~10%) in the present investigation. The perturbation pulse of very large intensity is naturally capable of destroying completely the stationary pattern of flow past a body even in the region of stability.

Typical patterns of the regimes are illustrated in Fig. 4, which presents the function $\rho(n)/\rho_\infty$ (M_∞ = 10, $Re_\infty = 0.25 \cdot 10^5$, Pr = 0.72, thermal insulation, $t = n\tau$, n is the number of the calculation step in time, τ = 0.1). The stable regime is presented in Fig. 4a (γ = 1.13). It is seen that after the passage of the first pulse (see [2]) the perturbed field of the flow undergoes a rapid relaxation, and the stationary pattern of flow past the body is recovered. We note that one and the same pattern of flow is recovered irrespective of the variation of the parameters that discretize the continuous differential problem, i.e., the number and configuration of the nodes of the computational grid and also of the starting conditions of the algorithm, and the numerical solution reaches the same branch; there are no bifurcations of the solution for all $\gamma > \gamma_1$. The rate of approach to the solution is almost the same over the entire computational domain.

The unstable regime is shown in Fig. 4b (γ = 1.03). Typical of this regime is the quasiperiodic, on the whole, evolution of perturbations. Curves 1, representing the function $\rho(t)$ at the stagnation point, make it possible to determine, with a sufficient degree of accuracy, the motion of the internal shock wave from the bow compression shock to the body, reflection from it, motion in the opposite direction from the body to the bow shock, etc. (for details, see [2]). Here, the peaks of density correspond to: the leading steep front corresponds to the instant of incidence of the internal shock wave on the nose part of the body, and the trailing front corresponds to the reflection of the shock wave from it. The reflected shock wave moves also downstream along the body surface and the bow shock, as is clearly seen from the evolution of curves 3 and 4, respectively. On a large time interval (the calculation was performed up to $n \sim 10^4$), the perturbations do not decay, and the stationary pattern of flow is not attained. With further decrease in γ, the perturbation incident on the bow shock destabilizes the flow completely, and it undergoes substantial reorganization. The front of the bow shock is destroyed completely or partially, and it is transformed into a compressing wave, similarly to that noted in [6]. Computation in the regime "external boundary of the computational domain is the front of the bow shock, the position and configuration of which is determined in the process of the solution of the whole problem" ([3, 4]), i.e., on the assumption of an "infinitely thin bow compression shock," leads to the failure of the algorithm, and the computation becomes impossible even when using mechanisms of the suppression of schematic instabilities.

In the range $\gamma_1 < \gamma < \gamma_3$, two characteristic regimes can be distinguished. Figure 4c ($\gamma = 1.1$) shows the neutrally stable regime. The perturbation passes downstream, and in the forward zone of the flow on the line of stagnation the stationary solution is attained rather rapidly ($n \sim 100$ at the forward point of the bow shock, curve 2; $n \sim 700$ at the stagnation point, curve 1). However, the analysis of the evolution of the parameters at the downstream point of the bow shock front (curve 4) points to aperiodic passage along the front of the bow shock of some "solitary waves," i.e., to oscillations of the shock surface (and correspondingly all the gas-dynamical parameters behind it). This picture closely resembles the picture of the emission of sound by a shock wave [7] at certain values of the parameters of the perturbation incident on its front. From the viewpoint of the theory of differential equations, the solution illustrated by curve 4 is typical not of the solution of the Navier–Stokes-type equations, but rather of the solutions to the equations of the type of Korteweg–de Vries [8] in the form of solitary solutions or a train of solution waves and also of the Euler gas-dynamical equations in the presence of force interactions of electric and gravitation types, which leads to soliton-like solutions [9]. The simultaneous consideration of curves 2 and 4, which correspond to the evolution of the parameters at the front of the bow shock "from above" and "from below" downstream, allows one to conclude the following: since at the "upper" point 2 (see Fig. 1) the solution is completely stationary and at the "lower" point 4 soliton-like waves are well developed (their intensity attains ~20% of the mean values at this point), at the front of the bow shock a point must exist (or an extended region) of generation of aperiodic perturbations. The analysis of the evolution of the parameters in the perturbed region of flow showed that the perturbation source is located in the vicinity of the point of intersection of the sonic line in the flow, on which the values of the local Mach number are equal to 1, with the bow shock front. The physical mechanism underlying the generation of a perturbation in this region is not clear enough as yet and requires further study. We note that numerical experiments on the elucidation of the effect of schematic parameters (grid, starting conditions, filters) confirmed a stable existence of this type of flow.

One more type of flow is a neutral regime with transition, as shown in Fig. 4d ($\gamma = 1.055$). This regime very much resembles the previous one in the evolution of perturbations in the forward region of flow. Perturbations rapidly decay and a stationary pattern develops: at the forward point of the bow shock toward the time step $n \sim 200$ (curve 2) and at the stagnation point toward $n \sim 1000$. Thereafter, here the gas-dynamical parameters were preserved with a high, up to 10^{-4}, degree of accuracy during the entire time of the numerical experiment. In the downstream region of flow (curves 3 and 4), the evolution pattern changes substantially. The perturbations of the type of solitary solitons are replaced by perturbations of an oscillatory type, which is closer to a periodic one. However, the main factor of this type of flow, which precisely determined the necessity of a separate description in the classification of regimes, is transition ($n \sim 4500$) from one solution to another, from a certain state "1" to another state "2," for example, for control point 4 from the value $\rho/\rho_\infty \approx 8$ to the value $\rho/\rho_\infty \approx 6.5$. It should be emphasized here that the transition became possible after, generally speaking, a long time of existence of a "nearly" stationary pattern of flow with a deviation of the solution from the mean one which does not exceed 10%. If the numerical experiment was stopped before the instant of time $n \sim 4500$, the phenomenon of transition would not be noted. The variation of the computational parameters demonstrated the stable presence of the effect of transition: a change in τ led to a corresponding change in n_*, so that the transition occurred at the same value of the physical time $t_* = n_*\tau$. With further continuation of the computation to the region of very large values of n, the picture remained the same oscillatory-quasistationary one as on the last portions of curves 3 and 4 of Fig. 4c (oscillations not higher than 10%). The reverse transition from state "2" to state "1" was never realized in numerical experiments; the transition occurred only in one direction ($\rho_2 < \rho_1$). The physical mechanism that caused this transition is not very clear and also requires further study. From the viewpoint of the theory of differential equations, this is the manifestation of the bifurcation nonuniqueness of the solutions of the Navier–Stokes system, and the value $\gamma = 1.055$ lies in the vicinity of the point of branching of solutions.

Some considerations are appropriate here. First, the closely coinciding numerical values for the "intensity" of the solitons and the "intensity" of the transition (defined as $|f_2 - f_1|/f_1$, where f_1 and f_2 are the initial and final states), of the order of 0.2, allow the assumption that, as a matter of fact, the "neutral regime" and "neutral regime with transition" are one and the same regime. The soliton-like behavior of the former is an "attempt" of one physical mechanism to realize transition of the solution from the first state to the second; however, the other mechanism returns the solution to the initial state. With decrease in γ from 1.07 to 1.055, the domination of the second mechanism is replaced by the domination of the first one with a corresponding transition.

To analyze the process, it is possible to utilize the theory of conical flow of a gas. It admits the existence of two types of solution (strong and weak) of the problem of supersonic flow impingement on a sharp cone with the formation of an attached compression shock. Even though in the present work we study supersonic flow past a blunt body with a detached bow shock, nevertheless the solutions of these two problems have much in common, especially outside the subsonic flow region, in the vicinity of the stagnation line. One is well aware of the relationship between the Mach number of a nonperturbed flow, the angle of flow deflection, and the angle of inclination of a compression shock that has two solutions, a strong and a weak one, i.e., the existence of two very different regimes of flow is possible (from the standpoint of gas dynamics). The strong solution is characterized by the turn of the supersonic free stream at a jump with its retardation to a subsonic one, while the weak one is characterized by the turn of the flow and preservation of the supersonic flow velocity behind the front of the shock. As is known, even though analysis from the standpoint of thermodynamics and statistical physics excludes neither of these two states, nevertheless it prefers the weak solution (with a smaller inclination angle of the shock and correspondingly with a smaller change of the parameters at the shock that converts the supersonic flow to a supersonic one with a small region of a subsonic flow). Precisely this solution is realized in the majority of physical and computational experiments. Moreover, attempts to obtain a strong solution in numerical experiments (see review [10]) or to retain it by having put it as an initial condition failed: either the algorithm pushed the data along the weak branch of the solution or the strong solution passed immediately, for several "steps" of the algorithm, into a weak one.

One of the regimes obtained in the present work (Fig. 4d) may be interpreted, with some caution, as transition from an analog of a "strong" solution to an analog of a "weak" one, with the "strong" solution existing for a rather long interval of algorithmic solution, and this effect reveals itself only in a very narrow interval of the governing parameters; in the present case, these are M_∞ and γ in the relationship $\gamma(M_\infty)$ that determines the limit of stability (see [1]).

Discussion of the Problem. Generally speaking, the discussion was begun above, when the results obtained were described and commented upon. However, it is pertinent to consider briefly a number of fundamental aspects of the nonuniqueness of numerical solutions as the reflection of the problem of the nonuniqueness of the solutions of differential equations (numerous theoretical works concerned with bifurcation of analytical solutions of nonlinear equations deal with the problem in a somewhat different way).

To illustrate, we consider a one-dimensional equation of transfer:

$$\frac{\partial f}{\partial t} + a\,\frac{\partial f}{\partial x} = 0\,, \tag{1}$$

whose general solution falls within the class of functions of the type of a "running wave":

$$f = F\,(x - at)\,. \tag{2}$$

To obtain numerical solution of (1), we can apply, for example, the algorithm

$$\frac{f_i^{n+1} - f_i^n}{\tau} + a\,\frac{f_{i+1}^n - f_i^n}{\delta x} = 0\,. \tag{3}$$

The specific, in the present case explicit, algorithm (3) is given for the sake of definiteness of further reasonings, with the problems of stability, degree of approximation, etc. being of no importance; they are not considered and are not discussed here, while the unvoidable brevity of presentation leads to a certain mathematical incorrectness in the description of the transition from continuity to discreteness and back.

Analysis of the nonuniqueness and of the possibility of the appearance of singularities in numerical solution (3) will be carried out on the basis of the principles of the theory of differential approximations. Using the Taylor series expension, we have

$$f^{n+1} = f^n + \sum_{k=1}^{\infty} \frac{\tau^k}{k\,!}\left(\frac{\partial^k f}{\partial t^k}\right)^n,\quad f_{i+1} = f_i + \sum_{l=1}^{\infty} \frac{\delta x^l}{l\,!}\left(\frac{\partial^l f}{\partial x^l}\right)_i\,. \tag{4}$$

Substituting (4) into (3) and taking off the coordinate subscripts of space and time (i, n), we obtain a full differential approximation of scheme (3):

$$\sum_{k=1}^{\infty} \frac{\tau^{k-1}}{k\,!}\left(\frac{\partial^k f}{\partial t^k}\right) + a\,\sum_{l=1}^{\infty} \frac{\delta x^{l-1}}{l\,!}\left(\frac{\partial^l f}{\partial x^l}\right) = 0\,. \tag{5}$$

From (5) we obtain the first differential approximation (k = 1, l = 1)

$$\frac{\partial f}{\partial t} + a\,\frac{\partial f}{\partial x} = Q_1\,(\tau) + Q_2\,(\delta x)\,. \tag{6}$$

On discarding the terms O_1 and O_2 for $\tau \to 0$ and $\delta x \to 0$, Eq. (6) goes over into Eq. (1). Of course, these are the rudiments of the computational mathematics, which, however, are required for a further discussion of the problem.

The second differential approximations (3) can be written in three forms: (k = 1, l = 2), k = 2, l = 1), and (k = 2, l = 2), respectively:

$$\frac{\partial f}{\partial t} + a\,\frac{\partial f}{\partial x} + \frac{a\delta x}{2}\,\frac{\partial^2 f}{\partial x^2} = 0\,, \tag{7}$$

$$\frac{\partial f}{\partial t} + \frac{\tau}{2}\,\frac{\partial^2 f}{\partial t^2} + a\,\frac{\partial f}{\partial x} = 0\,, \tag{8}$$

$$\frac{\partial f}{\partial t} + \frac{\tau}{2}\,\frac{\partial^2 f}{\partial t^2} + a\,\frac{\partial f}{\partial x} + \frac{a\delta x}{2}\,\frac{\partial^2 f}{\partial x^2} = 0\,. \tag{9}$$

Here, the terms $O_1(\tau^2)$ and $O_2(\delta x^2)$ on the right-hand sides are replaced by zeros for clarity of the illustration. The next differential approximations are written out similarly. The solutions of Eqs. (7)–(9) already differ substantially from the solution of the initial equation (1), and it is not guaranteed at all that substantial condensing of the mesh (τ, δx) will ensure the striving of solutions (7)–(9) toward solution (1) in the form of a "traveling wave" (2) in the entire range of the parameters that determine the class of the problems. (We note that one of the tests of the numerical algorithms developed is the determination of the transport properties of the scheme by solving the transfer equation, i.e., from the evolution of the profile prescribed at the initial time instant for the signal the quality of the algorithm is determined; see, e.g., [11].) This is true only for smooth solutions. But if a flow has singularities such as shock waves or tangential and contact discontinuities, then "the order of approximation of any algorithm falls actually to the first one" [12] despite the formally high order of its differential approximation.

In particular, differential approximations (8)–(9) have the type of the Duffing equation for t; its solution, even despite the smallness of the coefficient of f_t'', is time-dependent; the frequency characteristics and the phase pattern may substantially differ from similar properties of solutions to the equations of evolution type (1) or (7) with the presence of only the first derivative in time f_t'. The deviations of the attractors of discrete representations of Eqs. (8)–(9) from the attractors of Eq. (1) by some parameters in certain ranges of their changes (in the present work these parameters are the efficient specific heat ratio γ and the Mach number M_∞) may have a resonance character of substantially narrow-band form. It may well be that the transient regime is the manifestation of a certain strange attractor as a certain set in the space of states that attract, in addition to unstable, also stable trajectories but with very small (by γ and M_∞) regions of attraction.

For more complex (than the transfer equations) systems of the type of Euler, Navier–Stokes, and Barnett, there correspond more complex differential approximations. At different values of the small parameters τ and δx, their numerical solutions can exhibit different properties: dissipative, dispersive, soliton-like, etc., since they are determined not by the initial differential equations of the type of, for example, Navier–Stokes equations, but the differential approximations of the algorithms that implement them of the type of Clairaut Burgers, Korteweg-de Vries equations, etc., and these properties manifest themselves in rather narrow ranges of schematic parameters, as a rule, when there is a sharp change in the character of the problem.

Despite the great number of works, the problem of the nonuniqueness of the solutions to the systems of nonlinear differential equations is not at all clear, especially as regards the analysis of the solutions of applied problems. This, to the same extent (if not to a greater one), relates to the nonuniqueness of the solutions of discrete problems that approximate a continuous one with one degree of accuracy or another. Here, the following classes of nonuniqueness of solutions can be distinguished — those differing by:

1) discrete grids (number of nodes and their configuration);

2) starting conditions for stationary problems that are solved by the time-dependent technique;

3) by organization of computations.

These three classes relate to one numerical algorithm. Of course, there is also a class of nonuniqueness for different algorithms, since for its own algorithm there naturally exists its own differential approximation. A brief characteristic of each of the classes follows.

The most widely known of these is the class of nonuniqueness with respect to discrete grids. Common in computational mathematics is the notion of "poor quality" of numerical solutions with insufficient number of computational nodes or cells; their increase uniquely favors an increase in the quality of the solution. However, an increase in the power of the computational technique and the possibility of using grids with up to 10^6 nodes also led to the reverse effect in some problems. Thus, for example (see review [13] and the references therein), the experiment with flow past sharp wing profiles in some regimes reveals the formation of two vortices: a large, clearly seen one, and a small-scale one. Calculation on a grid with a small number of nodes makes it possible to obtain the pattern of flow only with one large vortex. A substantial increase in the number of nodes helps reveal also the second vortex, but a further increase (by an order of magnitude) in the number of nodes of the grid again leads to the pattern of flow with one vortex. This seems to be caused by the domination of the properties of another differential approximation of an applied discrete algorithm.

To the class of the nonuniqueness of numerical solutions of stationary problems by the time-dependent technique obtainable in a number of gas-dynamical regimes one may relate the nonuniqueness, investigated in [14], that exhibits itself in the loss of symmetry of the solution in calculation of physically symmetric problems by completely symmetric numerical algorithms and that is revealed in using, for the same problem, different initial data (starting conditions of the algorithm). This can show up in conducting a series of calculations in the hysteresis of the solutions obtained (see, e.g., [3]). However, the hysteresis of regimes is manifested not only in computational, but also in experimental investigations. Thus, in [15] a detailed study was made of the hysteresis of the aerodynamic coefficients C_y and M_z by the angle of attack α of two objects: a wing with the profile NASA 0018 and of a model of a plane with a wing with a large aspect ratio. Measurements of the parameters with direct progress of the experiment (increase in α from value to value in the range from -3^o to $+30^o$ and in the reverse process (decrease of α in the same range of angles) showed the formation of a hysteresis loop of the values of $C_y(\alpha)$ and $M_z(\alpha)$. A further division of the step of the experiment over α demonstrated the presence of a stable region of hysteresis and the appearance of other branches of hysteresis with locally unstable inner boundaries. Analysis of the phenomenon from the point of view of the theory of catastrophes [16] showed that the power J of the bifurcation set is $J = 2$ for an ordinary hysteresis and $J = 4$ and $J = 6$ for a hysteresis with one or two inner branches, respectively.

Another type of nonuniqueness, whose study has been initiated at the present time, the nonuniqueness with respect to the process of organization of computations, is as follows. A stationary stably existing picture of flow is exposed to the action of a special perturbing factor. This factor can be represented by a single-moment pulse, as in the present work, or can be extended in time; here, of great importance is the form, duration, and intensity of the perturbing pulse. Thus, in [7] an artificially induced transition from a regular to a Mach type of reflection of the shock wave and vice versa, from the Mach type to a regular type is studied. The gas-dynamic theory admits in a small range the existence of both regular and Mach type at the same time set of governing parameters, similarly to a weak and strong solution of the problem of flow past a cone. In [17], a localized but sufficiently extended in time and space perturbing pulse is incident on the stationary picture of flow with a Mach or regular configuration (we note that in a linear approximation both of these configurations are stable against small perturbations). At certain parameters of it, the stationary configuration of one type can pass over into a stationary configuration of another type. It is found that the energy expenditure on transformation of the Mach pattern into a regular one is greater than that of transformation of the regular pattern into the Mach one, i.e., the Mach configuration can be considered as a more stable one in the region of the double solution, and the point of branching of the solutions has the property of "selective transmissivity." An alternative selection of an actually realized type of configuration can be implemented by resorting to some analytical considerations. Thus, in [18], where problems of the incidence shock wave on the interface between two gases with different physical properties is studied, actually problems of the branching of solutions are considered, i.e., the possibility of the existence, at these or other values of the parameters, of the Mach or regular types of shock-wave configurations.

What are the criteria for the selection of the different solutions obtained? As yet, it is difficult to answer this question uniquely. In symmetrical problems it is possible to organize the control of the obtained solution, since the violation of symmetry is quite evident. It is possible to carry out cycles of calculations for determining or even, if necessary, "removing" nonsymmetric solutions. The calculations of essential space problems, with the occurrence of a complex structure of flows and instability of shock waves of the type of Richtmeyer–Meshkov (see, e.g., [19]) not adaptable to a simple analysis lead to fundamental difficulties of selection in the case of nonuniqueness of the solution.

Probably the importance of the problem of nonuniqueness of the solution of a physical problem, of the differential problem that describes the latter, and of the discrete algorithm that implements it will increase with the development of computational techniques and the appearance of systems of parallel calculation that make it possible to attain a much higher level of numerical simulation.

This work was carried out with financial support from the Russian Foundation for Fundamental Research (projects 99-01-00514 and 00-07-90297).

NOTATION

E, energy; ρ, density; U, velocity; M, Mach number; Re, Reynolds number; Pr, Prandtl number; γ, specific heat ratio; R, radius of body bluntness; d, distance of the detachment of a shock from the body at the stagnation line; x, coordinate; δx, step of calculation over the coordinate x; T, periodicity; t, time; n, number of the step of calculation in time; τ, step of calculation in time; I, intensity; ω, frequency; k, wave number; L, wave length; J, power of bifurcation set; α, angle of attack, C_y, coefficient of buoyancy; M_z, pitching moment. Subscripts: ∞, values in a nonperturbed flow; $*$, critical or characteristic value; s, values at the front shock; b, values on the surface; n, time index; i, coordinate index of the grid node; min, minimum value; max, maximum value.

REFERENCES

1. G. A. Tarnavskii and S. I. Shpak, *Inzh.-Fiz. Zh.*, **73**, No. 2, 354–357 (2000).
2. G. A. Tarnavskii and S. I. Shpak, *Zh. Tekh. Fiz.*, **70**, Issue 3, 82–86 (2000).
3. V. M. Kovenya, G. A. Tarnavskii, and S. G. Chornyi, *Application of the Method of Splitting in Problems of Aerodynamics* [in Russian], Novosibirsk (1990).
4. M. K. Lebedeva, A. E. Medvedev, and G. A. Tarnavskii, *Avtometriya*, No. 5, 76–83 (1994).
5. G. A. Tarnavskii and S. I. Shpak, in: *Modeling in Mechanics* [in Russian], Krasnoyarsk (2000). Deposited at VINITI 06.06.2000, No. 1625, pp. 131–156.
6. G. I. Mishin, A. P. Bedin, N. I. Yushchenkova, G. E. Skvortsov, and A. P. Ryazin, *Zh. Tekh. Fiz.*, **51**, No. 11, 2315–2324 (1981).
7. L. D. Landau and E. M. Lifshits, *Theoretical Physics*, Vol. 6, *Hydrodynamics* [in Russian], Moscow (1986).
8. V. I. Karpman, *Nonlinear Waves in Dispersing Media* [in Russian], Moscow (1973).
9. M. Ya. Ivanov and L. V. Terent'eva, *Prikl. Mat. Mekh.*, **63**, Issue 2, 258–266 (1999).
10. R. L. Eggers and M. J. Lewis, *Aircraft*, **35**, No. 4, 647–649 (1998).
11. V. M. Goloviznin and A. A. Samarskii, *Mat. Modelir.*, **10**, No. 1, 86–114 (1998).
12. S. K. Godunov, *Reminiscences about Difference Schemes* [in Russian], Novosibirsk (1997).
13. X. Zhong, *Comput. Phys.*, **144**, 662–709 (1998).
14. Yu. P. Golovachev and N. V. Leont'eva, *Zh. Vychisl. Mat. Mat. Fiz.*, **40**, No. 4, 638–646 (2000).
15. S. V. Kabin, I. V. Kolin, V. K. Svyatodukh, V. L. Sukhanov, and D. V. Shukhovtsov, *Uch. Zap. TsAGI*, **30**, Nos. 3–4, 61–68 (1999).
16. R. Gilmore, *Applied Theory of Catastrophes* [Russian translation], Moscow (1984).
17. M. S. Ivanov, A. N. Kudryavtsev, and D. V. Khotyanovskii, *Dokl. Ross. Akad. Nauk*, **373**, No. 3, 332–336 (2000).
18. S. K. Andilevko, *Inzh.-Fiz. Zh.*, **72**, No. 2, 208–225 (1999); **72**, No. 3, 507–518 (1999); **73**, No. 4, 802–806 (2000).
19. O. M. Belotserkovskii, V. V. Demchenko, and A. M. Oparin, *Dokl. Ross. Akad. Nauk*, **354**, No. 2, 190–193 (1997).